

Serveur Académique Lausannois SERVAL serval.unil.ch

Author Manuscript

Faculty of Biology and Medicine Publication

This paper has been peer-reviewed but does not include the final publisher proof-corrections or journal pagination.

Published in final edited form as:

Title: Reducing α ENaC expression in the kidney connecting tubule induces pseudohypoaldosteronism type 1 symptoms during K⁺ loading.

Authors: Poulsen SB, Praetorius J, Damkier HH, Miller L, Nelson RD, Hummler E, Christensen BM

Journal: American journal of physiology. Renal physiology

Year: 2016 Feb 15

Volume: 310

Issue: 4

Pages: F300-10

DOI: 10.1152/ajprenal.00258.2015

In the absence of a copyright statement, users should assume that standard copyright protection applies, unless the article contains an explicit statement to the contrary. In case of doubt, contact the journal publisher to verify the copyright status of an article.

1 Reducing α ENaC expression in kidney connecting tubule
2 induces pseudohypoaldosteronism type 1 symptoms during K⁺
3 loading

4

5 **Søren Brandt Poulsen¹, Jeppe Praetorius¹, Helle H. Damkier^{1,2}, Lance Miller³,**
6 **Raoul D. Nelson³, Edith Hummler⁴ and Birgitte Mønster Christensen¹**

7 *¹Department of Biomedicine, Aarhus University, Denmark; ²Department of Cellular and*
8 *Molecular Medicine, University of Copenhagen, Denmark ³Department of Pediatrics, University*
9 *of Utah School of Medicine, United States of America; and ⁴Department of Pharmacology and*
10 *Toxicology, University of Lausanne, Switzerland*

11

12 Running head: Important role of ENaC in CNT

13

14

15

16 Correspondence: Birgitte Mønster Christensen, Department of Biomedicine, Aarhus
17 University, Wilhelm Meyers Allé 3, DK-8000 Aarhus C, Denmark (e-mail:
18 bmc@biomed.au.dk; phone: +45 87167629; fax: +45 87167102).

19 **ABSTRACT**

20

21 Genetic inactivation of the epithelial Na⁺ channel α -subunit (α ENaC) in the renal
22 collecting duct (CD) does not interfere with Na⁺ and K⁺ homeostasis in mice.
23 However, inactivation in the CD and a part of the connecting tubule (CNT) induces
24 autosomal recessive pseudohypoaldosteronism type 1 (PHA-1) symptoms already on
25 a standard diet. In the present study, we further examined the importance of α ENaC
26 in the CNT. Knock-out mice with α ENaC deleted primarily in a part of the CNT (CNT-
27 KO) were generated using *Scnn1a*^{lox/lox} mice and *Atp6v1b1::Cre* mice. On a standard
28 diet, plasma [Na⁺] and [K⁺], and urine Na⁺ and K⁺ output were unaffected. Seven days
29 of Na⁺ restriction (0.01% Na⁺) led to a higher urine Na⁺ output only on day 3–5, and
30 after 7 days plasma [Na⁺] and [K⁺] were unaffected. By contrast, the CNT-KO mice
31 were highly susceptible to a 2-day 5% K⁺ diet and showed lower food intake and
32 relative body weight, lower plasma [Na⁺], higher fractional excretion (FE) of Na⁺,
33 higher plasma [K⁺], and lower FE of K⁺. The higher FE of Na⁺ coincided with lower
34 abundance and phosphorylation of the Na⁺-Cl⁻ cotransporter, NCC. In conclusion,
35 reducing ENaC expression in CNT induces clear PHA-1 symptoms during high dietary
36 K⁺ loading.

37

38

39 **KEYWORDS**

40

41 α ENaC, aldosterone, kidney connecting tubule, sodium, potassium

42 INTRODUCTION

43

44 The functional epithelial Na⁺ channel (ENaC) consists of the 3 homologous subunits,
45 α-, β-, and γ (3). Renal ENaC mediates Na⁺ reabsorption across the apical plasma
46 membrane of late distal convoluted tubule (DCT2) cells, connecting tubule (CNT)
47 cells, and collecting duct (CD) principal cells (17). Furthermore, ENaC-facilitated K⁺
48 secretion through apical K⁺ channels in the CNT and the cortical CD (CCD) may be
49 crucial for maintaining K⁺ homeostasis (10). During conditions of hypotension and
50 hyperkalemia, high angiotensin II or K⁺ plasma levels stimulate adrenal glomerulosa
51 cells to release the steroid hormone, aldosterone (33). The DCT2/early CNT are
52 largely insensitive to aldosterone, which is in contrast to the late CNT/CCD, where
53 ENaC activity is markedly increased by aldosterone (18, 23).

54 Loss-of-function mutations in any ENaC subunit may lead to the life-threatening
55 disease, autosomal recessive pseudohypoaldosteronism type 1 (PHA-1). PHA-1 is
56 characterized by, e.g., hyponatremia and hyperkalemia due to impaired ability of the
57 kidney to reabsorb Na⁺ and excrete K⁺ (4). We have in previous studies generated
58 various αENaC knock-out (KO) mouse lines contributing to an improved
59 understanding of the PHA-1 disease and the physiological importance of the ENaC
60 complex. Global αENaC inactivation is highly critical, leading to neonatal death (12).
61 Inactivation of αENaC in the CD and a part of the CNT (CNT/CD-KO) induces mild
62 hyponatremia on a standard diet and in addition serious weight loss during Na⁺
63 restriction (5). By contrast, CD-specific αENaC KO (CD-KO) mice are unaffected both
64 during Na⁺ restriction and high dietary K⁺ loading (28). Finally, conditional
65 inactivation of αENaC in the colon (colon-KO) induces fecal Na⁺ wasting but this is
66 compensated by the kidney and Na⁺ homeostasis is therefore not impaired (19).
67 Hence, these studies collectively point towards a critical role of αENaC particularly in
68 the DCT2 and CNT.

69 In the present study, we further examined the importance of αENaC in the CNT.
70 KO mice with αENaC deleted primarily in the CNT (CNT-KO) were generated using
71 *Scnn1a*^{lox/lox} mice (13) and *Atp6v1b1::Cre* mice. The latter mice have previously been
72 shown to express Cre recombinase in intercalated cells and in approximately 50% of

73 the CNT cells (20). This correlates with weak V-ATPase B1-subunit expression in
74 some CNT cells (1, 21). We performed a thorough characterization of the
75 *Atp6v1b1::Cre* mouse line by crossing it with an enhanced green fluorescent protein
76 (EGFP) reporter mouse line. The CNT-KO mice and the control littermates were
77 examined on standard and challenging diets.

78

79 **METHODS**

80

81 *Breeding of CNT-KO mice and control littermates, and Cre/EGFP reporter mice*

82

83 The Cre/loxP recombination system was utilized to investigate the role of ENaC
84 in the CNT for Na⁺ and K⁺ balance. We used a transgenic mouse line (genetic
85 background: C57BL/6J) in which exon 1 of the gene encoding the α -subunit of ENaC
86 (*Scnn1a*) was flanked by loxP sites [*Scnn1a*^{lox/lox} (13)]. The *Scnn1a*^{lox/lox} mouse line
87 was crossed with a mouse line (genetic background: C57Bl6/CBA) expressing Cre
88 recombinase under the regulatory elements of the *Atp6v1b1* gene (*Atp6v1b1::Cre*)
89 encoding the V-ATPase B1-subunit (20). The *Atp6v1b1::Cre* mouse line was also
90 recently utilized to inactivate aquaporin-2 genetically in the CNT (16). Interbreeding
91 of *Scnn1a*^{lox/lox} and heterozygous *Atp6v1b1::Cre* mice generated *Scnn1a*^{lox/+};
92 *Atp6v1b1::Cre* mice, which were further crossed to generate *Scnn1a*^{lox/lox};
93 *Atp6v1b1::Cre* mice. Finally, the *Scnn1a*^{lox/lox};*Atp6v1b1::Cre* mice were crossed with
94 *Scnn1a*^{lox/lox} mice to generate CNT-KO mice (*Scnn1a*^{lox/lox};*Atp6v1b1::Cre*) and control
95 littermates (*Scnn1a*^{lox/lox}). The mice were kept on a pelleted mouse chow standard
96 diet (Altromin Spezialfutter GmbH & Co. KG, Lage, Germany) in regular cages at 20°C.
97 Genotyping was carried out by running PCR analyses of tail biopsies using the
98 primers: *Scnn1a* (forward) 5'-CTC AAT CAG AAG GAC CCT GG-3', *Scnn1a* (forward):
99 5'-GTC ACT GTG TGC ACC CTT AA-3', and *Scnn1a* (reverse): 5'-GCA CAA AGA TCT TAT
100 CCA CC-3', *Cre* (forward): 5'-GTT CGC AAG AAC CTG ATG GAC-3', and *Cre* (reverse)5'-
101 CTA GAG CCT GTT TTG CAC GTT-3' (13).

102 In order to examine Cre recombinase activity in the *Atp6v1b1::Cre* line, these
103 mice were crossed with a dsRed/Cre-inducible EGFP reporter line [B6.Cg-Tg(CAG-
104 DsRed,-EGFP)5Gae/J; The Jackson Laboratory, Bar Harbor, Maine, USA].

105

106 *Experimental protocols*

107

108 A mixed population of male and female mice was studied [body weight (BW)
109 CNT-KO mice: 22.9 ± 0.4 g, $n = 64$; BW control mice: 22.6 ± 0.4 g, $n = 60$; $P = 0.383$].
110 For metabolic experiments, mice were kept in individual metabolic cages
111 (Techniplast, Buguggiate, Italy) at 27°C and initially fed a 3-day specialized standard
112 diet (0.25% Na⁺/0.7% K⁺; Altromin Spezialfutter GmbH & Co. KG, Lage, Germany). On
113 day 3, baseline parameters were recorded (BW, food intake, water intake, and urine
114 output) after which the mice were put on either a 4-day 0.01% Na⁺ diet (age: 10-15
115 weeks; for immunolabeling only), 7-day 0.01% Na⁺ diet (age: 13–28 weeks, two
116 experiments pooled), 4-day 2% K⁺ diet (age: 12–25 weeks), or a 2-day 5% K⁺ diet
117 (age: 10–37 weeks; two experiments pooled) or a or a 5% K⁺/0.01% Na⁺ diet (age: 5–
118 25 weeks; two experiments pooled). The diets were given as a mixture of food and
119 water [37.5% water (w/w)]. The added water was included in the total water intake.
120 For experiments in regular cages (blood sampled on standard diet; two experiments
121 were pooled for aldosterone measurements), mice were kept in individual cages at
122 20°C and fed a pelleted mouse chow diet for 7 days (Altromin Spezialfutter GmbH &
123 Co. KG). Mice had free access to food and water for the duration of all experiments. On
124 the last experimental day, mice were anesthetized by isoflurane inhalation, and blood
125 and tissue were collected. All experimental protocols complied with the European
126 Community guidelines for the use of experimental animals and were performed in
127 agreement with a license issued by the Animal Experiments Inspectorate, Ministry of
128 Food, Agriculture and Fisheries, Danish Veterinary and Food Administration.

129 *Collection and analyses of urine and blood*

130

131 Urine was collected in metabolic cages and cleared by centrifugation at 1000 *g* for
132 4 min, and concentrations of Na⁺ and K⁺ were measured using an IL943™ flame
133 photometer (Instrumentation Laboratory, Bedford, MA, USA; range Na⁺ and K⁺: 0–200
134 mM; QC: standards). Blood was collected through the portal vein using a 0.6 x 25 mm
135 needle containing 5 µl Li⁺ heparin solution and transferred to heparin-coated
136 centrifuge tubes (PST™ LH Tubes; BD, Franklin Lakes, NJ, USA) and immediately
137 centrifuged at 12,000 *g* for 4 min. Plasma concentrations of Na⁺ and K⁺ were
138 measured by MRC Harwell (Oxfordshire, UK) and determined using an ion selective
139 electrode (AU680; Beckman Coulter, Brea, CA, USA; range Na⁺: 50–200 mM; range K⁺:
140 1.0–10.0 mM, QC: standards). Plasma aldosterone concentrations were determined
141 using an enzyme immunoassay kit (EIA-5298; DRG International Inc., Springfield, NJ,
142 USA; range: 20–1000 pg/ml; QC: standards). Osmolality of urine and plasma was
143 measured using a freezing point depression osmometer (Advanced® Model 3320
144 Micro-Osmometer; Advanced Instruments, Inc., Norwood, MA, USA; range: 0–2000
145 mOsm/kg; QC: standards). Urinary NGAL [neutrophil gelatinase-associated lipocalin;
146 a biomarker for acute kidney injury (AKI) (7, 15)] concentrations were measured
147 using a mouse NGAL ELISA kit (Kit 042, Bioporto Diagnostics, Hellerup, Denmark).
148 Samples exceeding the upper limits of the test procedures were diluted according to
149 the manufacturers' protocols.

150

151 *Immunolabeling*

152

153 Mice were perfusion fixed via the left ventricle with 3% (v/v) paraformaldehyde
154 in PBS (pH 7.4), where after tissue was post fixed for 1 hour at 4°C. Subsequently, the
155 tissue was gradually dehydrated in ethanol, incubated in xylene, and embedded in
156 paraffin. Using a previously described standard protocol (26), paraffin embedded
157 kidney and colon sections (2 µm) from CNT-KO mice and control mice were labeled
158 with primary αENaC rabbit antibody (28), dilution 1:800). Paraffin-embedded kidney
159 sections from the Cre/EGFP reporter mice were labeled with NCC SPC-402D rabbit

160 primary antibody (StressMarq Biosciences Inc. Victoria, BC, Canada; dilution 1:200),
161 calbindin (D28K - 10R-C106A) mouse primary antibody (Fitzgerald Industries
162 International, Concord, MA, USA; dilution 1:20.000), AQP2 7661 rabbit primary
163 antibody ((24), dilution 1:1000), and EGFP goat primary antibody (ab6673, Abcam,
164 Cambridge, UK; dilution 1:1000). For light microscopy, immunolabeling was
165 visualized using peroxidase-conjugated goat anti-rabbit secondary antibody (p448;
166 Dako, Glostrup, Denmark; dilution 1:200) and 3,3'-diaminobenzidine (Kem-EN-Tec
167 Diagnostics A/S, Tåstrup, Danmark). For fluorescence microscopy, immunolabeling
168 was visualized using the secondary antibodies (dilution 1:600) donkey anti-goat 488
169 (Molecular Probes, Life Technologies), donkey anti-rabbit 555 (Molecular Probes, Life
170 Technologies), and donkey anti-mouse 633 (Molecular Probes, Life Technologies).

171

172 *Microscopy*

173

174 Counting of α ENaC-positive cells in CNT/DCT2 (in cortical labyrinth), and CCD (in
175 medullary arrays) was performed on kidney sections from CNT-KO mice and control
176 mice directly in the microscope (400x magnification). Only cells with a distinct
177 nucleus and apical α ENaC labeling were counted. Furthermore, counting was only
178 performed on cells situated in tubules with a clear visible luminal space and with at
179 least one α ENaC-positive cell in the tubule. The total number of cells counted in the
180 cortical labyrinth were 345 in the CNT-KO mice ($n = 5$) and 402 in the control mice (n
181 $= 5$). The total number of cells counted in medullary arrays were 86 in the CNT-KO
182 mice ($n = 5$) and 70 in the control mice ($n = 5$). The fraction of α ENaC-positive cells
183 was calculated from the number of α ENaC-positive cells divided by the total number
184 of cells counted in each animal. Imaging of kidney and distal colon sections was
185 carried out using a Leica DMRE light microscope equipped with a digital camera
186 (Leica, Wetzlar, Germany). Imaging of kidney and distal colon sections from
187 Cre/EGFP reporter mice ($n = 2$) were performed using a Leica TCS SL laser scanning
188 confocal microscope and Leica confocal software (Leica). Images were merged using
189 Image J software (Image J, Bethesda, MD, USA). Counting of EGFP-positive cells in the
190 CNT and DCT2 was performed on confocal images taken from Cre/EGFP mice

191 reporter mice, which were labeled for EGFP, calbindin and NCC ($n = 2$ animals, one
192 slide from each animal). The images were taken with a 63x objective. The fraction of
193 EGFP-positive CNT cells (strongly calbindin-positive/NCC-negative) was calculated
194 from the number of EGFP-positive/strongly calbindin-positive/NCC-negative cells
195 divided by the total number of strongly calbindin-positive/NCC-negative cells. The
196 fraction of EGFP-positive DCT2 cells (calbindin- and NCC-positive) was calculated
197 from the number of EGFP-positive/calbindin- and NCC-positive cells divided by the
198 total number of calbindin- and NCC-positive cells. The total number of cells counted
199 in the CNT were 132 ($n = 2$) and 64 in the DCT2 ($n = 2$).

200

201 *Semi-quantitative immunoblotting*

202

203 Tissue was collected, dissected on ice, and immediately homogenized at 4°C in
204 dissection buffer containing protease and phosphatase inhibitors. The homogenates
205 were centrifuged at 1000 g for 10 min at 4°C. The supernatants were supplemented
206 with sample buffer to a final concentration of 0.1 M SDS and heated to 65° C for 15
207 min. Samples were run on Criterion™ TGX™ Precast Gels (4–15% or Any kD; Bio-Rad
208 Laboratories, Hercules, CA, USA) and transferred by electroelution to PVDF
209 membranes (Bio-Rad Laboratories, Hercules, CA, USA) or Hybond-P PVDF
210 membranes (GE Healthcare, Little Chalfont, UK). Subsequently, the membranes were
211 blocked and incubated overnight at 4°C with primary rabbit antibodies [α ENaC (30),
212 dilution 1:1000; NKCC2 1495 (9, 14), dilution 1:50; pT96-T101-NKCC2 9934, (6)
213 dilution 1:250]; NCC SPC-402D, dilution 1:1000; pT53-NCC 1246 (25), dilution 1:250;
214 pT58-NCC 1251 (25), dilution 1:1000; or Anti-Kir1.1 (ROMK1) (Alomone, Jerusalem,
215 Israel; dilution 1:400)]. Labeling was visualized using the Enhanced
216 Chemiluminescence system (GE Healthcare, Little Chalfont, UK) or SuperSignal West
217 Femto Chemiluminescent Substrate (Thermo Scientific, Rockford, IL, USA). Because
218 aldosterone might regulate housekeeping genes such as actin, Coomassie-stained gels
219 were used to correct quantification for deviations in protein loading. The maximal
220 deviations in total protein concentration between samples on individual blots were \pm
221 10%.

222 *Statistical analyses*

223

224 Data meeting statistical assumptions of normality and variance homogeneity were
225 analyzed using Students two-sided *t*-test, while data only meeting assumptions of
226 normality were analyzed using Satterthwaite's two-sided unequal variance *t*-test.
227 Data not meeting assumptions of normality were ln-transformed or square-root
228 transformed in accordance with Sokal and Rohlf (29), and analyzed using the
229 appropriate *t*-tests. If data did not fulfill assumptions of normality after
230 transformation, untransformed data were analyzed using Mann-Whitneys U-test. For
231 parameters where the CNT-KO mice and control mice were compared at multiple
232 time points, *P*-values were adjusted using FDR correction (22). Tests were carried out
233 using Stata 12.0 (StataCorp, College Station, TX, USA) for Windows. All values are
234 presented as mean \pm SE.

235

236 **RESULTS**

237

238 *Evaluation of CNT-KO mice*

239

240 Breeding of CNT-KO mice and control mice followed Mendelian inheritance (50%
241 *Scnn1a*^{lox/lox}; *Atp6v1b1::Cre* and 50% *Scnn1a*^{lox/lox}, *n* = 204). Using single
242 immunolabeling, counting of α ENaC-positive cells in the cortical labyrinth (no
243 discrimination was made between CNT and DCT2) identified α ENaC expression in
244 approximately 45% of the cells in the CNT-KO mice, whereas in the control mice the
245 fraction was approximately 70% (Fig. 1A, B and E). This corresponded to
246 approximately 40% fewer α ENaC-positive cells in the CNT-KO mice (*P* < 0.001). In the
247 CCD (medullary arrays), the CNT-KO mice showed a weak tendency towards fewer
248 α ENaC-positive cells (9%; *P* = 0.217; Fig. 1C, D, and E). The overall lower fraction of
249 α ENaC-positive cells coincided with immunoblotting of cortical/outer medullary
250 (OM) tissue showing 55% lower total protein intensity of α ENaC in the CNT-KO mice
251 [both cleaved (30 kD) and full length (90 kD), *P* < 0.001, Fig. 1F and G]. Cre
252 recombinase activity in the DCT2 was examined by crossing the *Atp6v1b1::Cre* mice

253 with an dsRed/inducible enhanced green fluorescent protein (EGFP) reporter line
254 (Fig. 2 and 3). The progeny expressed EGFP in only a minor portion of the DCT2 cells
255 (approximately 6% [5% and 7%, respectively, in the 2 mice], Fig. 2A–C), whereas the
256 majority of DCT2 cells were EGFP-negative (Fig. 3A–C). This indicated that a potential
257 deletion of α ENaC in the DCT2 was minimal. Consistent with the lower number of
258 α ENaC-positive cells in the CNT-KO, the EGFP reporter mouse expressed EGFP in a
259 high number of the CNT cells (Fig. 2D–I), while EGFP was absent in the majority of
260 CCD principal cells (Fig. 2J–L and 3D–F). Cellular counting revealed that
261 approximately 36% of the CNT cells ([32% and 39%, respectively, in the 2 mice],
262 identified as strongly calbindin-positive and NCC-negative) expressed EGFP. Thus,
263 characterization of the mice indicated that α ENaC was inactive primarily in a part of
264 the CNT cells.

265

266 *Distal colonic α ENaC expression was not impaired in the CNT-KO mice.*

267

268 ENaC is an important mediator of Na⁺ reabsorption in the surface epithelial layer
269 of the distal colon (8, 19). It was previously reported that the *Atp6v1b1::Cre* mice
270 show unspecific Cre recombinase activity in the colon (20). This could potentially
271 cause inactivation of α ENaC in the distal colon of the CNT-KO mice. The Cre/EGFP
272 reporter mice showed no detectable EGFP expression in the surface epithelial layer or
273 in the crypts (Fig. 4A). However, some cells in the connective tissue expressed EGFP
274 (Fig. 4A, arrows), indicating Cre recombinase activity. We further tested whether
275 α ENaC expression was impaired in the distal colon of the CNT-KO mice by using
276 immunolabeling and immunoblotting. Immunolabeling detected α ENaC in the surface
277 epithelial layer of both CNT-KO mice and control mice kept on a 4-day 0.01% Na⁺ diet
278 (Fig. 4B and C). Immunoblotting demonstrated that the abundance of total α ENaC
279 [(cleaved (30 kD) + full length (90 kD))] did not differ between CNT-KO mice and
280 control mice kept on the 7-day 0.01% Na⁺ diet [$P = 0.512$; Fig. 4 and E]. However, the
281 30 kD/90 kD ratio was higher in the CNT KO mice [$P = 0.017$, Fig. 4D and E],
282 suggesting greater cleavage of α ENaC and thus, increased activity [reviewed in (27)].
283 A non-regulated band was found at 55 kD [CNT-KO mice: 1.00 ± 0.08 ($n = 9$), control

284 mice: 1.00 ± 0.22 ($n = 9$), $P = 0.986$, Fig. 4D and E], but whether this was a cleaved
285 form of α ENaC was not further examined. Collectively, data demonstrated that α ENaC
286 expression was not impaired in the distal colon of the CNT-KO mice.

287

288 *Phenotyping of CNT-KO mice on standard and challenging diets.*

289

290 To examine the effect of genetic α ENaC inactivation in the CNT on Na^+ and K^+
291 homeostasis, CNT-KO mice and control mice were examined on a standard diet
292 (baseline), 7-day 0.01% Na^+ diet, 4-day 2% K^+ diet, a 2-day 5% K^+ diet, or a 5%
293 K^+ /0.01% Na^+ diet.

294

295 *Standard diet.* When fed a standard diet in regular cages, no differences were found in
296 plasma [Na^+], [K^+], creatinine concentration, or osmolality between CNT-KO mice and
297 control mice (Fig. 5A, B, D and E). However, the plasma aldosterone concentration
298 was higher in the CNT-KO mice ($P < 0.01$, Fig. 5C). Baseline measurements in
299 metabolic cages did not show any differences in the tested parameters [relative body
300 weight (BW), food intake, water intake, urine output, urine Na^+ and K^+ output, and
301 urine osmolality; Fig. 6A–U]. Similarly, no significant differences in these parameters
302 were observed when pooling baseline data (collected over the last 24 h prior to diet
303 manipulation) from the metabolic cage experiments (data not shown).

304

305 *Seven-day 0.01% Na^+ diet.* Challenging the CNT-KO mice with a 7-day 0.01% Na^+ diet
306 did not affect plasma [Na^+], [K^+], creatinine concentration, or osmolality (Fig. 5A, B, D
307 and E), however, the plasma aldosterone concentration was still higher compared to
308 the control mice ($P < 0.01$, day 7, Fig. 5C). On day 3–5, the CNT-KO mice excreted
309 more Na^+ in the urine than the control mice (P between 0.01 and 0.05; Fig. 6E),
310 however, the difference diminished on day 6 and eventually disappeared on day 7
311 [not significant (NS), Fig. 6E]. The urine osmolality was higher in the CNT-KO mice on
312 day 4 and 7 ($P < 0.05$, Fig. 6G) compared to the control mice, whereas no differences
313 were found in relative BW, food intake, water intake, urine output, and urine K^+
314 excretion (Fig. 6A–D and F).

315

316 *Four-day 2% K⁺ diet.* When challenged with a 4-day 2% K⁺ diet, plasma [Na⁺], [K⁺],
317 creatinine concentration, and osmolality (Fig. 5A, B, and D) did not differ between the
318 CNT-KO mice and the control mice, however, the plasma aldosterone concentration
319 was clearly higher (day 4: $P < 0.001$, Fig. 5C). By contrast, no differences were found
320 in relative BW, food and water intake, urine output, urine Na⁺ and K⁺ output, and
321 urine osmolality (Fig. 6H–N).

322

323 *Two-day 5% K⁺ diet.* The 2-day 5% K⁺ diet induced a lower relative BW in the CNT-KO
324 mice compared to the control mice (day 1: $P < 0.001$; day 2: $P < 0.001$; Fig. 6O), which
325 was accompanied by lower plasma [Na⁺] (day 2: $P < 0.001$, Fig. 5A). The total urine
326 Na⁺ output was unaffected (NS, Fig. 6S), however, the CNT-KO mice consumed less
327 food (and thereby less Na⁺) than the control mice (day 1: $P < 0.001$; day 2: $P < 0.01$;
328 Fig. 6P). This was taken into account by calculating the Na⁺ output (urine)/intake
329 (food) ratio. The Na⁺ output/intake ratio was higher in the CNT-KO mice compared to
330 the control mice on both day 1 ($P < 0.001$, Table 1) and day 2 ($P < 0.01$, Table 1).
331 Furthermore, the fractional excretion (FE) of Na⁺ was higher in the CNT-KO mice
332 when measured on day 2 ($P < 0.01$, Table 1). In terms of K⁺ homeostasis, the CNT-KO
333 mice presented higher plasma [K⁺] (day 2: $P < 0.001$, Fig. 5B) and lower urine K⁺
334 output (day 1: $P < 0.001$, day 2: $P < 0.05$, Fig. 6T) compared to the control mice, but
335 the K⁺ output/intake ratio was not different, neither on day 1 nor day 2 (NS, Table 1).
336 However, the FE of K⁺ was lower in CNT-KO mice when measured on day 2 ($P < 0.05$,
337 Table 1), indicating impaired K⁺ excretion. Finally, the CNT-KO mice showed higher
338 plasma aldosterone concentration (day 2: $P < 0.001$, Fig. 5C), creatinine concentration
339 ($P < 0.01$, Table 1), and lower glomerular filtration rate (GFR; $P < 0.05$, Table 1), water
340 intake (day 1: $P < 0.01$, Fig. 6Q), and urine output (day 1: $P < 0.05$, Fig. 6R) than the
341 control mice. NGAL concentrations were measured in urine samples collected on day
342 2. There were no significant differences in urinary NGAL concentrations [CNT-KO
343 mice: 150.8 ± 52.4 ng/ml ($n = 10$), control mice: 85.8 ± 35.4 ng/ml ($n = 8$), $P = 0.131$]
344 or in urinary NGAL excretion [CNT-KO mice: 32.0 ± 11.6 ng/g BW/24 h ($n = 10$),
345 control mice: 16.6 ± 6.8 ng/g BW/24 h ($n = 8$), $P = 0.248$].

346 Mice were, furthermore, tested on a 2-day 5% K⁺/0.01% Na⁺ diet. The control
347 mice showed lower relative BW both on day 1 ($P < 0.001$) and day 2 ($P < 0.001$)
348 compared to baseline, suggesting that BW loss during K⁺ loading was not specific for
349 the CNT-KO mice, but could be induced in control mice when combining K⁺ loading
350 and Na⁺ restriction. However, the weight loss was less severe in the control mice
351 compared to the CNT-KO both on day 1 (control: 0.96 ± 0.01 , $n = 10$; KO: 0.91 ± 0.00 , n
352 $= 10$; $P < 0.001$) and day 2 (control: 0.94 ± 0.01 , $n = 10$; KO: 0.86 ± 0.01 , $n = 10$; $P <$
353 0.001).

354

355 *The CNT-KO mice presented lower abundance and phosphorylation of NCC on a 5% K⁺*
356 *diet*

357

358 Hyperkalemia is connected with reduced Na⁺ reabsorption in the thick ascending
359 limb (TAL) and the distal convoluted tubule (DCT), leading to increased Na⁺ delivery
360 to ENaC-expressing tubular segments thereby favoring K⁺ secretion (30, 31, 34, 35).
361 Therefore, we tested whether the higher FE of Na⁺ in the CNT-KO mice compared to
362 the control mice during K⁺ loading occurred in parallel with lower protein abundance
363 and phosphorylation of the Na⁺-K⁺-2Cl⁻ cotransporter, NKCC2 (expressed in TAL), and
364 the Na⁺-Cl⁻ cotransporter, NCC (expressed in DCT). Immunoblotting of cortical/OM
365 tissue (collected on day 2) showed no differences in the protein abundances of
366 NKCC2, pT96-T101-NKCC2, or the pT96-T101-NKCC2/NKCC2 ratio (NS, Fig. 7). By
367 contrast, we found a lower abundance of total NCC ($P < 0.05$, Fig. 7), pT53-NCC ($P <$
368 0.01 , Fig. 7), and pT58-NCC ($P < 0.001$, Fig. 7). Furthermore, the pT53-NCC/NCC ($P <$
369 0.05 , Fig. 7) and the pT58-NCC/NCC ratios ($P < 0.001$, Fig. 7) were lower in the CNT-
370 KO mice, suggesting that the lower phosphorylation of NCC was not a result of lower
371 total NCC protein abundance *per se*. Finally, no effect was found on ROMK abundance
372 (Fig. 7). Collectively, the higher FE of Na⁺ in the CNT-KO mice fed a 5% K⁺ diet
373 coincided with lower abundance and phosphorylation of NCC in the DCT and lower
374 α ENaC expression in the CNT.

375 **DISCUSSION**

376

377 This study provides novel insight into the physiological role of α ENaC in the
378 kidney and the activation of compensatory mechanisms in a conditional model of the
379 PHA-1 syndrome. CNT-KO mice showed a severe phenotype when examined on a 5%
380 K^+ diet as evidenced by e.g. higher plasma $[K^+]$ and lower FE of K^+ . This could be a
381 result of impaired ENaC-mediated K^+ secretion in CNT through apical K^+ channels
382 such as ROMK (2). Although the CNT-KO mice were unable to maintain K^+ balance to
383 the same extent as the controls, data indicated that compensatory mechanisms did
384 take place. The mice presented higher plasma aldosterone level and lower abundance
385 and phosphorylation of the DCT-specific Na^+ transporter, NCC, indicating lower Na^+
386 reabsorption in the DCT. Inhibition of Na^+ reabsorption in the TAL and the DCT
387 during hyperkalemia may lead to higher tubular flow rate and Na^+ delivery to ENaC-
388 expressing tubule segments (30, 31, 34, 35), producing a favorable gradient for K^+
389 secretion in the CNT and CCD. Thus, a compensatory target in our model could be
390 NCC in the DCT. By contrast, we did not observe a significantly lower abundance or
391 phosphorylation of NKCC2, which is vital for Na^+ reabsorption in the TAL and macula
392 densa. Another potential compensatory target is ROMK, but our data did not show
393 any changes in ROMK abundance either.

394 On the 5% K^+ diet, lower NCC activity, together with inactivation of α ENaC in the
395 CNT, coincided with higher FE of Na^+ and Na^+ output/intake ratio in the CNT-KO mice.
396 Importantly, this suggests that in the CNT-KO mice, ENaC in the CD was not sufficient
397 to effectively reabsorb a higher Na^+ delivery. Collectively, these events may have
398 induced the lower plasma $[Na^+]$ in the CNT-KO mice. To exclude that the phenotype
399 could be a result of AKI, urinary NGAL concentrations were determined on day 2. The
400 lack of differences in both urinary NGAL concentration and excretion as well as the
401 lack of differences in urine output and water intake between the CNT-KO mice and
402 the control mice on day 2 indicated that the CNT-KO mice had not developed AKI. We
403 did not observe any difference in total urinary Na^+ output after 1 and 2 days of 5% K^+
404 loading, however, it cannot be excluded that a potential difference in Na^+ output could
405 be detected at earlier time points (i.e. after minutes) (30).

406 The CNT-KO mice presented higher aldosterone levels on the low-Na⁺ diet and a
407 mild phenotype as evidenced by Na⁺ wasting on day 3–5. However, this effect
408 eventually disappeared after 7 days, after which no effects were found on plasma
409 [Na⁺] and [K⁺]. Data indicated higher cleavage of ENaC in the distal colon and this
410 potential activation of ENaC could, at least partially, have compensated for reduced
411 renal Na⁺ reabsorption in the CNT.

412 We have previously shown that genetic inactivation of αENaC in the CD did not
413 interfere with Na⁺ and K⁺ balance in mice kept on a standard diet, low-Na⁺ diet, or a
414 6% K⁺ diet (28). This suggests that αENaC in the CD is apparently not a prerequisite
415 for maintaining Na⁺ and K⁺ homeostasis. By contrast, combined αENaC inactivation in
416 a part of the CNT (approximately 30% fewer αENaC-positive cells in early CNT, and
417 70% fewer αENaC-positive cells in late CNT) and CD induced PHA-1 symptoms
418 already on a standard diet as evidenced by natriuresis, hyponatremia, and
419 hyperkalemia (5). During Na⁺ restriction, the CNT/CD-KO mice showed lower relative
420 BW, severe urine Na⁺ loss, hyponatremia, and hyperkalemia (5). Thus, the phenotype
421 was stronger in the CNT/CD-KO mice than in the CNT-KO mice on a standard diet or a
422 low-Na⁺ diet. Besides a potential compensation in the colon, it is possible that the CD
423 in the CNT-KO mice could partially compensate for the lack of αENaC in the CNT.
424 Because αENaC was deleted in the CD of the CNT/CD-KO mice, such compensation
425 was not possible in these mice. However, it cannot be ruled out either that the
426 deletion of αENaC in the CNT-KO was less efficient than in the CNT/CD-KO mice
427 thereby explaining the milder phenotype. Thus, it is possible that the remaining CNT
428 cells still expressing αENaC in the CNT-KO were sufficient to maintain proper Na⁺
429 balance.

430 A 5% K⁺ diet induced a weaker phenotype in the CNT/CD-KO mice than in the
431 CNT-KO mice. Both mouse lines showed lower plasma [Na⁺] and higher plasma [K⁺]
432 on the 5% K⁺ diet, however, the CNT-KO mice additionally presented lower food
433 intake and lower relative BW, whereas these parameters were unaffected in the
434 CNT/CD-KO mice. Impaired ENaC-facilitated K⁺ secretion in the colon (11, 32), was
435 not likely to cause the stronger phenotype in the CNT-KO mice, because the colonic
436 αENaC expression was intact. Although the role of ENaC in the DCT2 for K⁺ secretion

437 is unknown, it could be speculated that deletion of α ENaC only in a few DCT2 cells
438 could become critical during K^+ loading.

439 In summary, we examined the importance of α ENaC in the CNT by generating KO
440 mice in which α ENaC was deleted primarily in the CNT. The mice showed no obvious
441 phenotype on a standard diet, 0.01% Na^+ diet, or a 2% K^+ diet. The elevated
442 aldosterone levels in the CNT-KO mice may stimulate ENaC activity in the late CNT (in
443 remaining ENaC expressing cells), in the CD, or in the colon and potentially
444 compensate for the reduced Na^+ reabsorption in the CNT. On a 5% K^+ diet, however,
445 the mice presented clear PHA-1 symptoms. Our data provide an unprecedented
446 insight into compensatory mechanisms taking place in a conditional model of the
447 PHA-1 syndrome. Even when α ENaC is deleted only in a part of the CNT, several
448 compensatory mechanisms occur. During 5% K^+ loading, this includes higher plasma
449 aldosterone level, lower renal NCC activity, and lower GFR. Clinically, the results may
450 contribute to a deeper understanding of how the body copes with the physiological
451 challenges that are taking place in PHA-1 patients.

452

453 **ACKNOWLEDGMENTS**

454

455 The antibodies against α ENaC, and pT53-NCC and pT58-NCC used for semi-
456 quantitative immunoblotting were kindly provided by J. Loffing (Institute of Anatomy,
457 University of Zurich, Switzerland) and R. Fenton (Department of Biomedicine, Aarhus
458 University, Denmark), respectively. We thank J. Frøkiær (Department of Clinical
459 Medicine, Aarhus University Hospital, Aarhus, Denmark) for help on measuring urine
460 $[Na^+]$ and $[K^+]$, and I. M. S. Paulsen, H. Høyer, C. Westberg, T. Drejer, P. A. Nielsen, and
461 M. S. Gandry for technical assistance.

462

463 **GRANTS**

464

465 Funding for this study was provided by the Danish Council for Independent
466 Research (B.M.C.), the Lundbeck Foundation (B.M.C.), the Danish Heart Foundation
467 (B.M.C.), and Health (Faculty of Health Sciences, Aarhus University; S.B.P.).

468 **DISCLOSURES**

469

470 None.

471

472 **AUTHOR CONTRIBUTIONS**

473

474 S.B.P.: conception and design of the experiments; collection, analysis, and
475 interpretation of data; drafting the article or revising it critically for important
476 intellectual content; J.P.: drafting the article or revising it critically for important
477 intellectual content; H.H.D.: collection of data; drafting the article or revising it
478 critically for important intellectual content; L.M.: drafting the article or revising it
479 critically for important intellectual content; R.D.N.: drafting the article or revising it
480 critically for important intellectual content; E.H.: drafting the article or revising it
481 critically for important intellectual content; B.M.C.: conception and design of the
482 experiments; collection, analysis, and interpretation of data; drafting the article or
483 revising it critically for important intellectual content; All authors approved the final
484 version of the manuscript.

485

486

487 **REFERENCES**

488

489 1. **Alper SL, Natale J, Gluck S, Lodish HF and Brown D.** Subtypes of intercalated
490 cells in rat kidney collecting duct defined by antibodies against erythroid band
491 3 and renal vacuolar H⁺-ATPase. *Proc Natl Acad Sci U S A* 86: 5429-5433, 1989.

492 2. **Arroyo JP, Ronzaud C, Lagnaz D, Staub O and Gamba G.** Aldosterone
493 paradox: differential regulation of ion transport in distal nephron. *Physiology*
494 *(Bethesda)* 26: 115-123, 2011.

495 3. **Canessa CM.** Structural biology: unexpected opening. *Nature* 449: 293-294,
496 2007.

497 4. **Chang SS, Grunder S, Hanukoglu A, Rosler A, Mathew PM, Hanukoglu I,**
498 **Schild L, Lu Y, Shimkets RA, Nelson-Williams C, Rossier BC and Lifton RP.**
499 Mutations in subunits of the epithelial sodium channel cause salt wasting with
500 hyperkalaemic acidosis, pseudohypoaldosteronism type 1. *Nat Genet* 12: 248-
501 253, 1996.

502 5. **Christensen BM, Perrier R, Wang Q, Zuber AM, Maillard M, Mordasini D,**
503 **Malsure S, Ronzaud C, Stehle JC, Rossier BC and Hummler E.** Sodium and
504 potassium balance depends on alphaENaC expression in connecting tubule. *J*
505 *Am Soc Nephrol* 21: 1942-1951, 2010.

- 506 6. **Dimke H, Flyvbjerg A, Bourgeois S, Thomsen K, Frokiaer J, Houillier P,**
507 **Nielsen S and Frische S.** Acute growth hormone administration induces
508 antidiuretic and antinatriuretic effects and increases phosphorylation of
509 NKCC2. *Am J Physiol Renal Physiol* 292: F723-F735, 2007.
- 510 7. **Doi K, Katagiri D, Negishi K, Hasegawa S, Hamasaki Y, Fujita T, Matsubara**
511 **T, Ishii T, Yahagi N, Sugaya T and Noiri E.** Mild elevation of urinary
512 biomarkers in prerenal acute kidney injury. *Kidney Int* 82: 1114-1120, 2012.
- 513 8. **Duc C, Farman N, Canessa CM, Bonvalet JP and Rossier BC.** Cell-specific
514 expression of epithelial sodium channel alpha, beta, and gamma subunits in
515 aldosterone-responsive epithelia from the rat: localization by in situ
516 hybridization and immunocytochemistry. *J Cell Biol* 127: 1907-1921, 1994.
- 517 9. **Ecelbarger CA, Terris J, Hoyer JR, Nielsen S, Wade JB and Knepper MA.**
518 Localization and regulation of the rat renal Na⁽⁺⁾-K⁽⁺⁾-2Cl⁻ cotransporter, BSC-
519 1. *Am J Physiol* 271: F619-F628, 1996.
- 520 10. **Giebisch G.** Renal potassium transport: mechanisms and regulation. *Am J*
521 *Physiol* 274: F817-F833, 1998.
- 522 11. **Grotjohann I, Gitter AH, Kockerling A, Bertog M, Schulzke JD and Fromm**
523 **M.** Localization of cAMP- and aldosterone-induced K⁺ secretion in rat distal
524 colon by conductance scanning. *J Physiol* 507: 561-570, 1998.

- 525 12. **Hummler E, Barker P, Gatzky J, Beermann F, Verdumo C, Schmidt A,**
526 **Boucher R and Rossier BC.** Early death due to defective neonatal lung liquid
527 clearance in alpha-ENaC-deficient mice. *Nat Genet* 12: 325-328, 1996.
- 528 13. **Hummler E, Merillat AM, Rubera I, Rossier BC and Beermann F.**
529 Conditional gene targeting of the Scnn1a (alphaENaC) gene locus. *Genesis* 32:
530 169-172, 2002.
- 531 14. **Jensen AM, Norregaard R, Topcu SO, Frokiaer J and Pedersen M.** Oxygen
532 tension correlates with regional blood flow in obstructed rat kidney. *J Exp Biol*
533 212: 3156-3163, 2009.
- 534 15. **Kawano H, Muto S, Ohmoto Y, Iwata F, Fujiki H, Mori T, Yan L and Horie S.**
535 Exploring urinary biomarkers in autosomal dominant polycystic kidney
536 disease. *Clin Exp Nephrol* 2014.
- 537 16. **Kortenoeven ML, Pedersen NB, Miller RL, Rojek A and Fenton RA.** Genetic
538 ablation of aquaporin-2 in the mouse connecting tubules results in defective
539 renal water handling. *J Physiol* 591: 2205-2219, 2013.
- 540 17. **Loffing J and Kaissling B.** Sodium and calcium transport pathways along the
541 mammalian distal nephron: from rabbit to human. *Am J Physiol Renal Physiol*
542 284: F628-F643, 2003.

- 543 18. **Loffing J, Zecevic M, Feraille E, Kaissling B, Asher C, Rossier BC, Firestone**
544 **GL, Pearce D and Verrey F.** Aldosterone induces rapid apical translocation of
545 ENaC in early portion of renal collecting system: possible role of SGK. *Am J*
546 *Physiol Renal Physiol* 280: F675-F682, 2001.
- 547 19. **Malsure S, Wang Q, Charles RP, Sergi C, Perrier R, Christensen BM,**
548 **Maillard M, Rossier BC and Hummler E.** Colon-specific deletion of epithelial
549 sodium channel causes sodium loss and aldosterone resistance. *J Am Soc*
550 *Nephrol* 25: 1453-1464, 2014.
- 551 20. **Miller RL, Lucero OM, Riemondy KA, Baumgartner BK, Brown D, Breton S**
552 **and Nelson RD.** The V-ATPase B1-subunit promoter drives expression of Cre
553 recombinase in intercalated cells of the kidney. *Kidney Int* 75: 435-439, 2009.
- 554 21. **Miller RL, Zhang P, Smith M, Beaulieu V, Paunescu TG, Brown D, Breton S**
555 **and Nelson RD.** V-ATPase B1-subunit promoter drives expression of EGFP in
556 intercalated cells of kidney, clear cells of epididymis and airway cells of lung in
557 transgenic mice. *Am J Physiol Cell Physiol* 288: C1134-C1144, 2005.
- 558 22. **Narum SR.** Beyond Bonferroni: less conservative analyses for conservation
559 genetics. *Conserv Genet* 7: 783-787, 2006.
- 560 23. **Nesterov V, Dahlmann A, Krueger B, Bertog M, Loffing J and Korbmacher**
561 **C.** Aldosterone-dependent and -independent regulation of the epithelial

562 sodium channel (ENaC) in mouse distal nephron. *Am J Physiol Renal Physiol*
563 303: F1289-F1299, 2012.

564 24. **Nielsen J, Kwon TH, Praetorius J, Frokiaer J, Knepper MA and Nielsen S.**
565 Aldosterone increases urine production and decreases apical AQP2 expression
566 in rats with diabetes insipidus. *Am J Physiol Renal Physiol* 290: F438-F449,
567 2006.

568 25. **Pedersen NB, Hofmeister MV, Rosenbaek LL, Nielsen J and Fenton RA.**
569 Vasopressin induces phosphorylation of the thiazide-sensitive sodium
570 chloride cotransporter in the distal convoluted tubule. *Kidney Int* 78: 160-169,
571 2010.

572 26. **Poulsen SB, Kim YH, Frokiaer J, Nielsen S and Christensen BM.** Long-term
573 vasopressin-V2-receptor stimulation induces regulation of aquaporin 4
574 protein in renal inner medulla and cortex of Brattleboro rats. *Nephrol Dial*
575 *Transplant* 28: 2058-2065, 2013.

576 27. **Rossier BC and Stutts MJ.** Activation of the epithelial sodium channel (ENaC)
577 by serine proteases. *Annu Rev Physiol* 71: 361-379, 2009.

578 28. **Rubera I, Loffing J, Palmer LG, Frindt G, Fowler-Jaeger N, Sauter D, Carroll**
579 **T, McMahon A, Hummler E and Rossier BC.** Collecting duct-specific gene

- 580 inactivation of alphaENaC in the mouse kidney does not impair sodium and
581 potassium balance. *J Clin Invest* 112: 554-565, 2003.
- 582 29. **Sokal RR and Rohlf FJ.** In: Biometry, edited by W.H.Freeman and Company.
583 New York: 1995.
- 584 30. **Sorensen MV, Grossmann S, Roesinger M, Gresko N, Todkar AP,**
585 **Barmettler G, Ziegler U, Odermatt A, Loffing-Cueni D and Loffing J.** Rapid
586 dephosphorylation of the renal sodium chloride cotransporter in response to
587 oral potassium intake in mice. *Kidney Int* 83: 811-824, 2013.
- 588 31. **Stokes JB.** Consequences of potassium recycling in the renal medulla. Effects
589 of ion transport by the medullary thick ascending limb of Henle's loop. *J Clin*
590 *Invest* 70: 219-229, 1982.
- 591 32. **Sweiry JH and Binder HJ.** Characterization of aldosterone-induced potassium
592 secretion in rat distal colon. *J Clin Invest* 83: 844-851, 1989.
- 593 33. **Thomas W and Harvey BJ.** Mechanisms underlying rapid aldosterone effects
594 in the kidney. *Annu Rev Physiol* 73: 335-357, 2011.
- 595 34. **Vallon V, Schroth J, Lang F, Kuhl D and Uchida S.** Expression and
596 phosphorylation of the Na⁺-Cl⁻ cotransporter NCC in vivo is regulated by

597 dietary salt, potassium, and SGK1. *Am J Physiol Renal Physiol* 297: F704-F712,
598 2009.

599 35. **van der Lubbe N, Moes AD, Rosenbaek LL, Schoep S, Meima ME, Danser**
600 **AH, Fenton RA, Zietse R and Hoorn EJ.** K⁺-induced natriuresis is preserved
601 during Na⁺ depletion and accompanied by inhibition of the Na⁺-Cl⁻
602 cotransporter. *Am J Physiol Renal Physiol* 305: F1177-F1188, 2013.

603 **FIGURE LEGENDS**

604

605 Fig. 1. α ENaC expression was lower in the CNT-KO mice. *A–D*, in mice kept on a 4-day
606 0.01% Na⁺ diet, immunolabeling showed more α ENaC-positive cells in the CNT/DCT2
607 (in the cortical labyrinth) of controls (*A*, arrows indicate α ENaC-positive cells) than in
608 the CNT-KO mice (*B*, arrow heads indicate α ENaC-negative cells). *E*, the fraction of
609 α ENaC-positive cells in the CNT/DCT2 was approximately 40% lower in the CNT-KO
610 mice, whereas no significant difference was found in the CCD (*C–E*, arrows indicate
611 α ENaC-positive cells, in medullary arrays). *F* and *G*, on a standard diet, the CNT-KO
612 mice showed 55% lower total α ENaC protein intensity in cortical/outer medullary
613 tissue homogenate [cleaved (30 kD) + full length (90 kD)]. Each bar indicates mean \pm
614 SE. ***P* < 0.01, ****P* < 0.001.

615

616 Fig. 2. *Atp6v1b1::Cre*/enhanced green fluorescent protein (EGFP) reporter mice
617 expressed EGFP in AQP2 and calbindin-positive cells in the CNT, whereas only a few
618 NCC-positive cells in the DCT2 and a few AQP2-positive cells in the CCD were EGFP
619 positive. Calbindin was used a marker for CNT/DCT2. *A–C*, arrow: NCC-
620 positive/EGFP-positive cell. *D–F*, arrow: calbindin-positive/EGFP-positive cell;
621 arrowhead: calbindin-negative/EGFP-positive cell; asterisk: calbindin-positive/EGFP-
622 negative cell. *G–I*, arrow: calbindin-positive/AQP2-positive/EGFP-positive cell;
623 arrowhead: AQP2-negative/EGFP-positive cell. *J–L*, arrow: AQP2-positive/EGFP-
624 positive cell; arrowhead: AQP2-negative/EGFP-positive cell; asterisk: AQP2-
625 positive/EGFP-negative cell. Glo: glomerulus.

626 Fig. 3. The majority of NCC-positive cells in the DCT2 and AQP2-positive cells in the
627 CCD did not express EGFP in the *Atp6v1b1::Cre*/EGFP reporter mice. *A–C*, arrowhead:
628 NCC-negative/EGFP-positive cell; asterisks: NCC-positive/EGFP-negative cells. *D–F*,
629 arrowhead: AQP2-negative/EGFP-positive cell; asterisks: AQP2-positive/EGFP-
630 negative cells.

631

632 Fig. 4. Distal colonic α ENaC expression was not impaired in the CNT-KO mice. *A*,
633 *Atp6v1b1::Cre/EGFP* reporter mice showed EGFP expression in some cells of the
634 connective tissue in the distal colon (arrows), whereas EGFP was not detectable in
635 the surface epithelial layer ($n = 2$). *B*, in the control mice and *C*, the CNT-KO mice kept
636 on a 4-day 0.01% Na⁺ diet, immunolabeling revealed clear apical labelling in the distal
637 colonic surface epithelial layer. *D* and *E*, immunoblotting and corresponding
638 densitometric analyses of distal colonic homogenates showed that total α ENaC
639 abundance (30+90 kD bands, arrows) did not differ between the control mice and the
640 CNT-KO mice kept on a 7-day 0.01% Na⁺ diet. The 30/90 kD-ratio was, however,
641 higher in the CNT-KO mice than in the control mice. Each bar indicates mean \pm SE. **P*
642 < 0.05. LU: lumen, CR: crypt.

643

644 Fig. 5. Blood parameters: the CNT-KO mice presented a clear phenotype on a 5% K⁺
645 diet. Effects of various diets on, *A*, plasma [Na⁺], *B*, plasma [K⁺], *C*, plasma aldosterone
646 concentration, *D*, plasma creatinine concentration, and, *E*, plasma osmolality in the
647 control mice and the CNT-KO mice. The mice were kept on either a standard diet in
648 regular cages ([Na⁺], [K⁺], creatinine and osmolality: control $n = 7$, KO $n = 9$;
649 aldosterone: control $n = 14$, KO $n = 17$), 7-day 0.01% Na⁺ diet in metabolic cages
650 ([Na⁺], [K⁺], aldosterone, and osmolality: control $n = 17$, KO $n = 18$; creatinine: control
651 $n = 15$, KO $n = 15$), 4-day 2% K⁺ diet in metabolic cages (control $n = 9$, KO $n = 9$), or a
652 2-day 5% K⁺ diet in metabolic cages (control $n = 8$, KO $n = 10$). Each bar indicates
653 mean \pm SE. ***P* < 0.01, ****P* < 0.001.

654

655 Fig. 6. Metabolic parameters: the CNT-KO mice presented a clear phenotype on a 5%
656 K⁺ diet. The control mice and the CNT-KO mice were kept in metabolic cages on a
657 standard diet (baseline) followed by either a, *A-G*, 7-day 0.01% Na⁺ diet (control $n =$
658 17–18, KO $n = 17$ –18), *H-N*, 4-day 2% K⁺ diet (control $n = 9$, KO $n = 9$), or, *O-U*, a 2-
659 day 5% K⁺ diet (*O-R*, control $n = 17$, KO $n = 18$; *S-U*, control $n = 9$, KO $n = 8$). Each
660 circle indicates mean \pm SE. **P* < 0.05, ***P* < 0.01, ****P* < 0.001.

661

662 Fig. 7. The CNT-KO mice presented lower abundance and phosphorylation of NCC on
663 a 5% K⁺ diet. Presented are protein abundances of NKCC2, p-NKCC2 (pT96/T101),
664 NCC, pT53-NCC, pT58-NCC, and ROMK in control mice (*n* = 8) and CNT-KO mice (*n* =
665 10) as determined by immunoblotting of cortical/outer medullary tissue
666 homogenates. Furthermore, presented are the ratios of pT96-T101-NKCC2/NKCC2,
667 pT53-NCC/NCC, and pT58-NCC/NCC. Each bar indicates mean ± SE. **P* < 0.05, ***P* <
668 0.01, ****P* < 0.001.

669

670 TABLES

Table 1. Urine and plasma parameters in control mice and CNT-KO mice kept on a 2-day 5% K⁺ diet

Parameter		Control			KO			<i>P</i>
		Mean	SE	<i>n</i>	Mean	SE	<i>n</i>	
Na ⁺ output/intake ratio	Baseline	0.73	0.07	9	0.71	0.06	8	NS
	day 1	0.98	0.05	9	1.47	0.07	8	< 0.001
	day 2	0.72	0.04	9	0.95	0.05	8	< 0.01
K ⁺ output/intake ratio	Baseline	0.72	0.05	9	0.66	0.06	8	NS
	day 1	0.73	0.03	9	0.60	0.04	8	NS
	day 2	0.69	0.03	9	0.70	0.04	8	NS
FE Na ⁺ (%)	day 2	0.42	0.03	8	0.56	0.03	10	< 0.01
FE K ⁺ (%)	day 2	71	7	8	51	5	10	< 0.05
Plasma creatinine (mM)	day 2	7.6	0.4	8	11.0	0.7	10	< 0.01
GFR (μl/min)	day 2	290	30	8	219	17	10	< 0.05

671

672

673

674

675

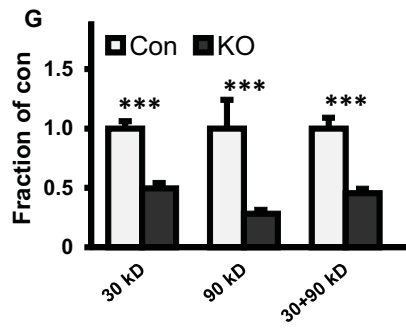
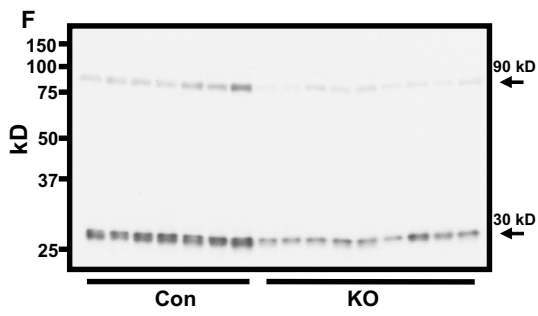
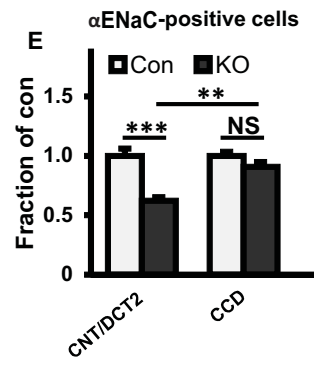
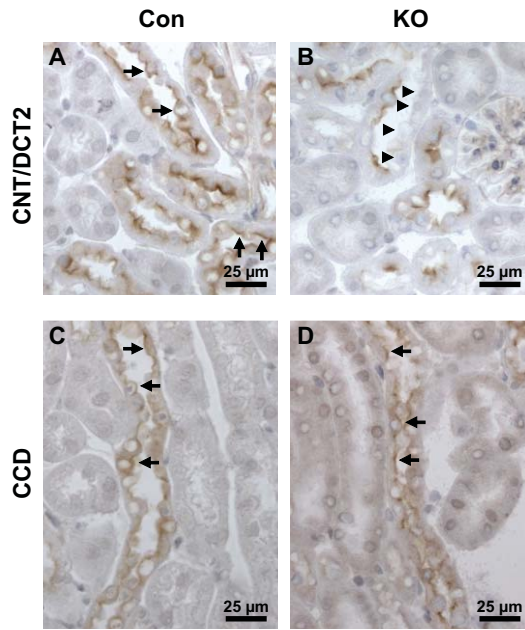
676

677

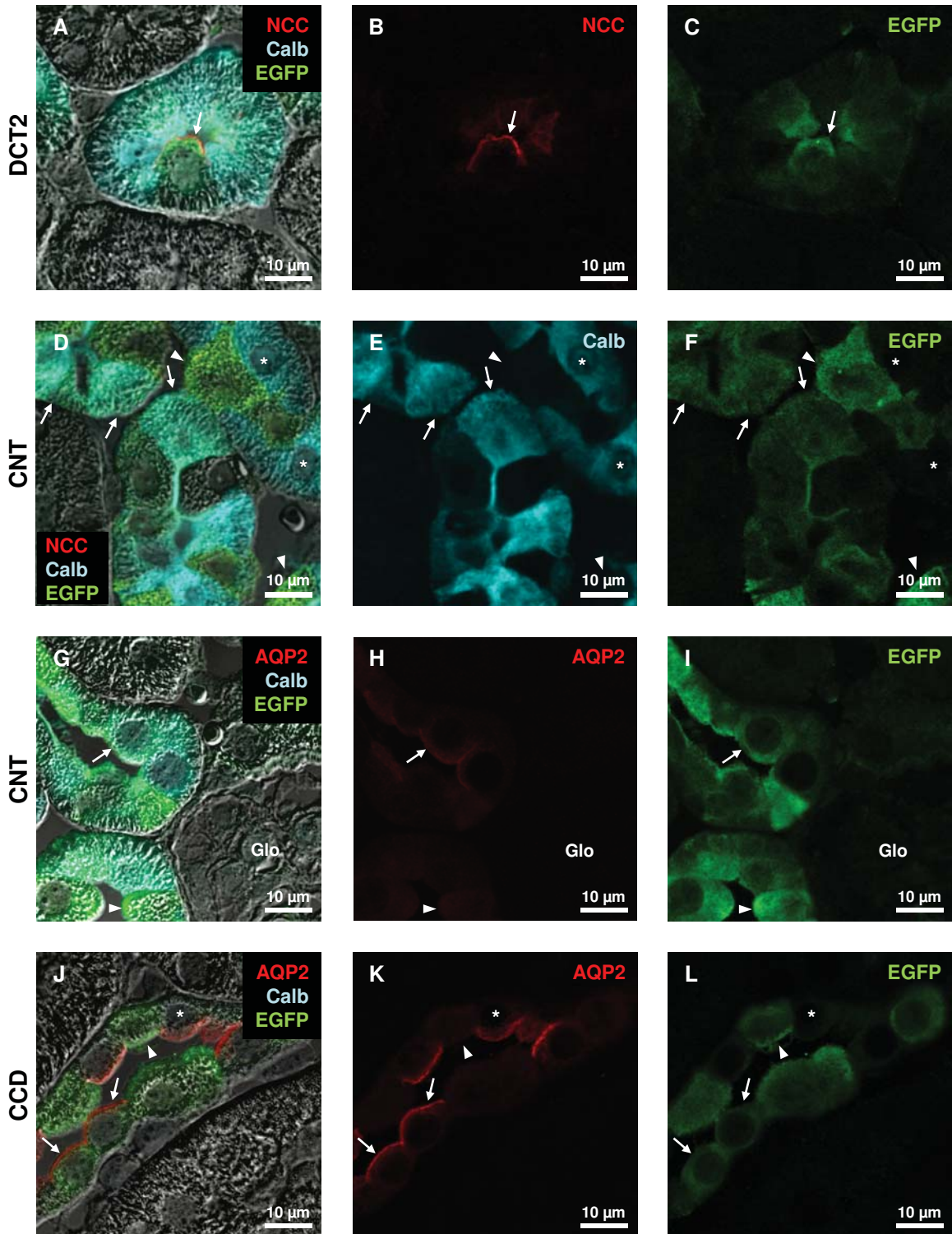
678

679

680



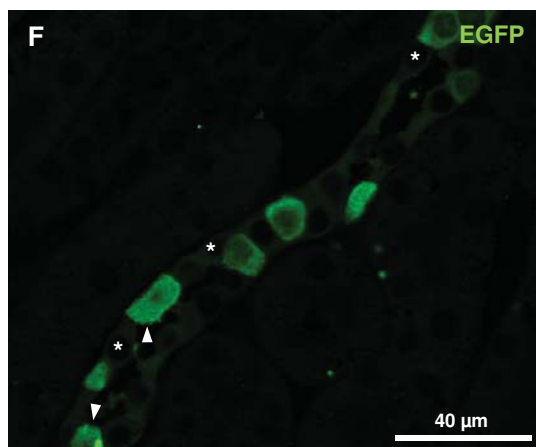
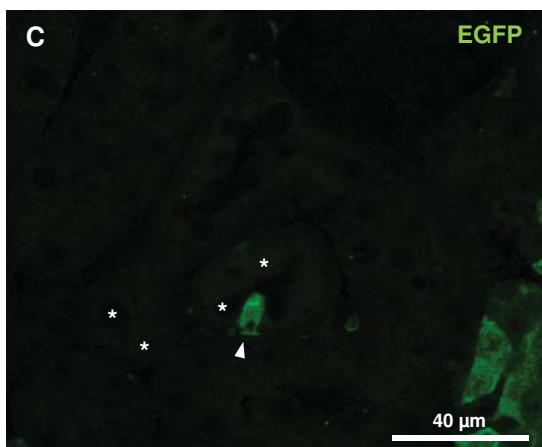
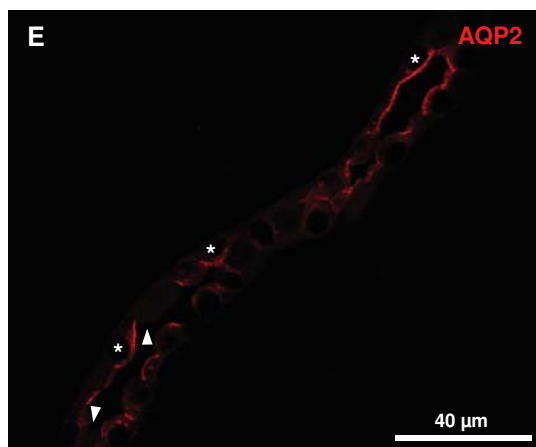
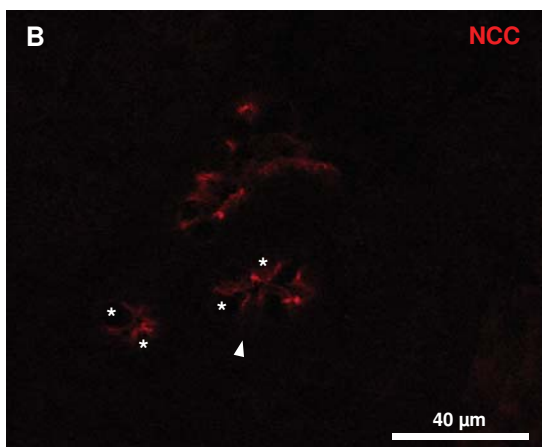
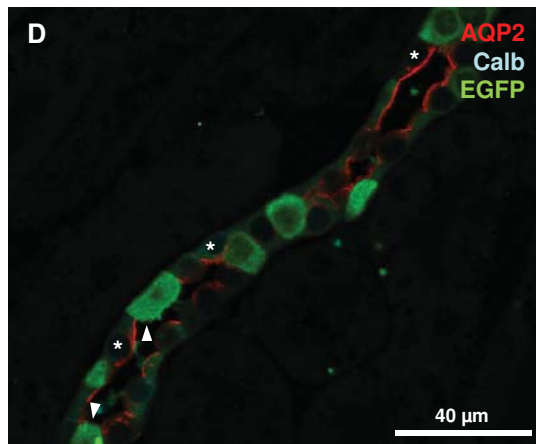
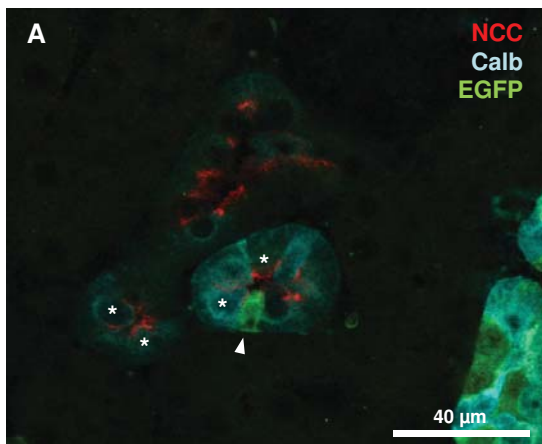
Cre/EGFP reporter mouse



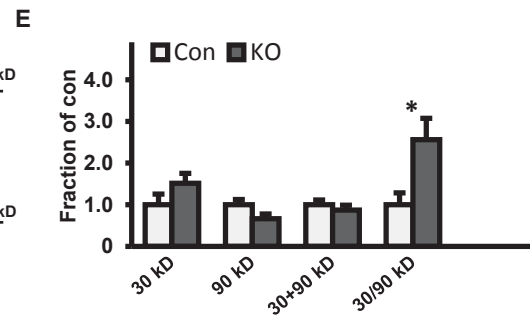
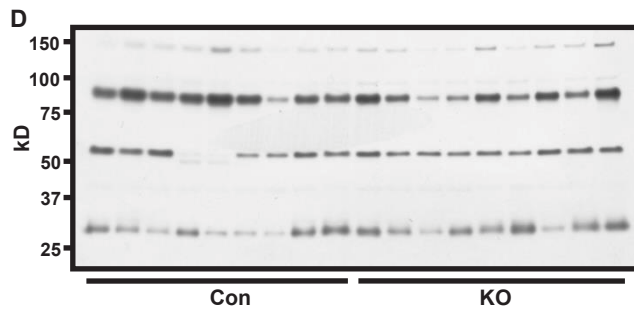
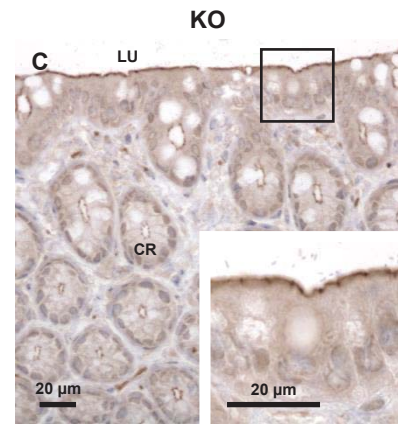
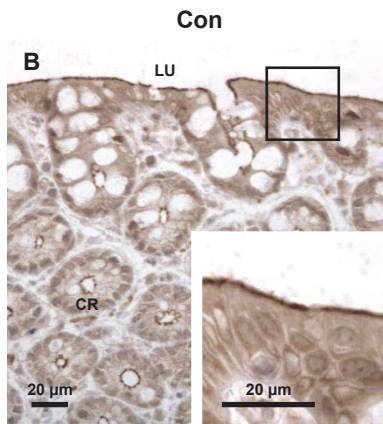
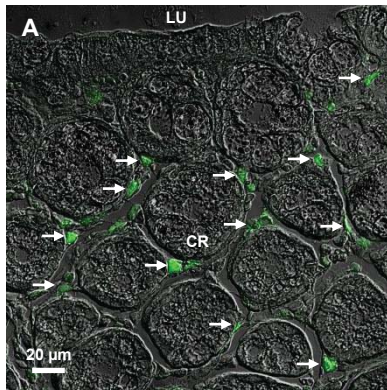
Cre/EGFP reporter mouse

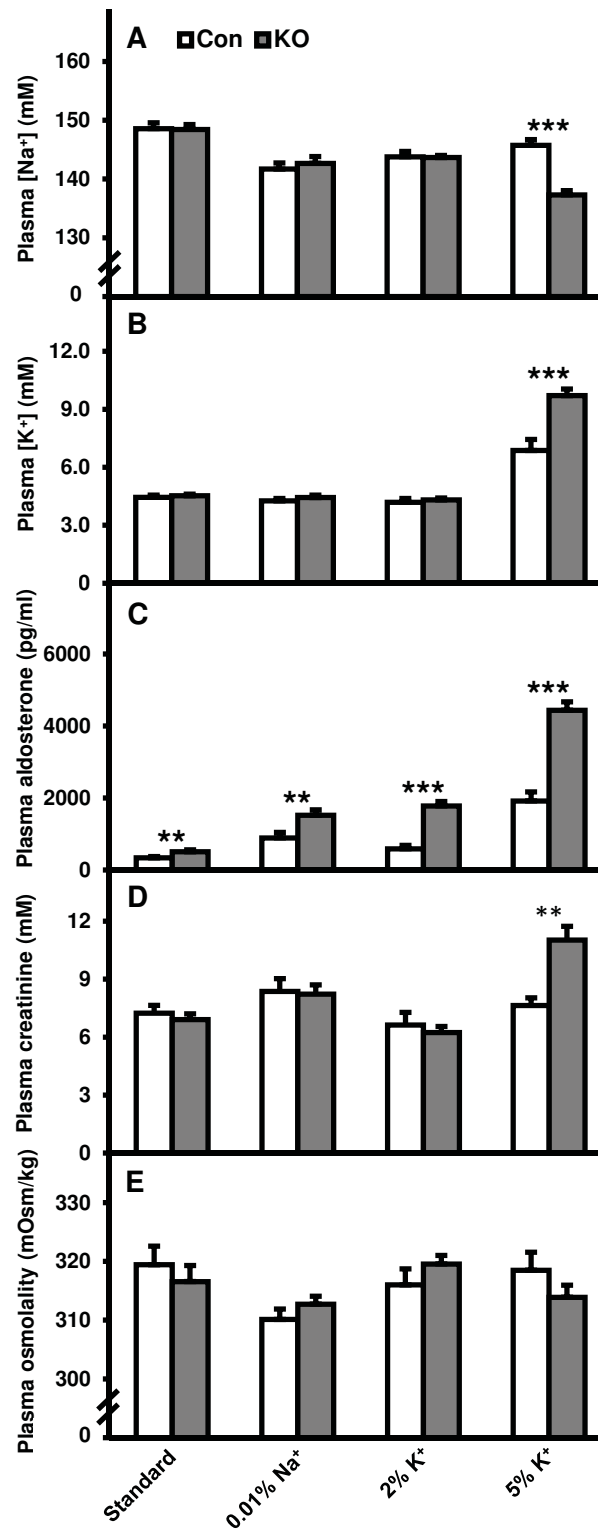
DCT2

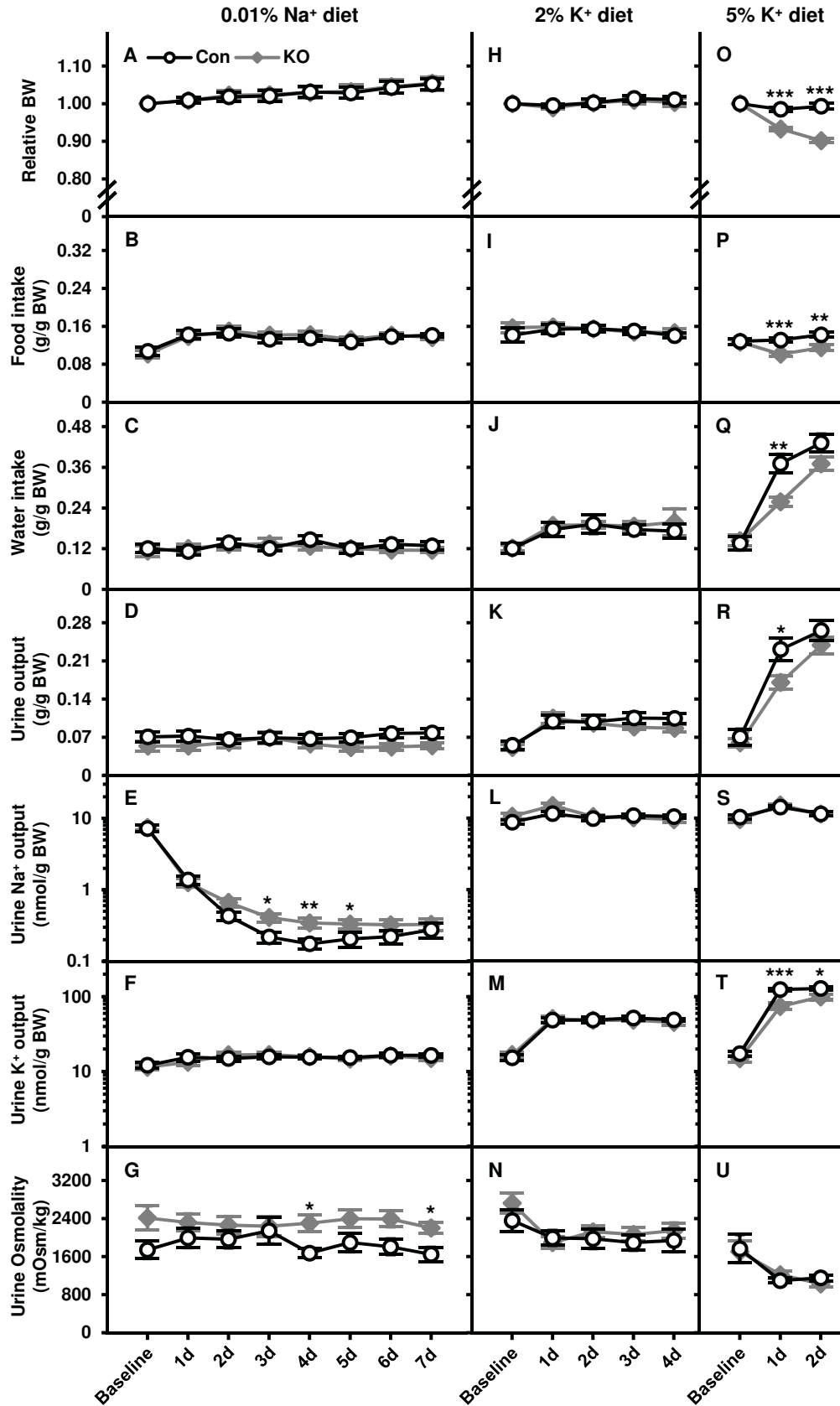
CCD



Cre/EGFP reporter mouse







5% K⁺ diet

